DMD Fast Forward. Published on April 4, 2011 as doi:10.1124/dmd.111.039107

DMD # 39107

Nonlinear Pharmacokinetics of 5-Methoxy-*N,N*-dimethyltryptamine in Mice

Hong-Wu Shen, Xi-Ling Jiang, Ai-Ming Yu

Department of Pharmaceutical Sciences, University at Buffalo, The State University of New York, Buffalo, NY 14260-1200, USA

DMD Fast Forward. Published on April 4, 2011 as DOI: 10.1124/dmd.111.039107
This article has not been copyedited and formatted. The final version may differ from this version.

DMD # 39107

Running Title: Nonlinear pharmacokinetics of 5-MeO-DMT

Address correspondence to: Dr. Ai-Ming Yu, Department of Pharmaceutical Sciences, School of Pharmacy and Pharmaceutical Sciences, University at Buffalo, The State University of New York, 541 Cooke Hall, Buffalo, NY 14260-1200, E-mail: aimingyu@buffalo.edu

Manuscript metrics:

Pages 20

Tables 3

Figures 6

References 39

Words in the Abstract 223

Words in the Introduction 616

Words in the Discussion 973

ABBREVIATIONS: 5-MeO-DMT, 5-methoxy-*N*,*N*-dimethyltryptamine; MAO-A, monoamine oxidase-A; CYP2D6, cytochrome P450 2D6; Tg-*CYP2D6*, *CYP2D6*-humanized; LC-MS/MS, liquid chromatography tandem mass spectrometry; C_{max}, maximum concentration; AUC, area under the curve; T_{max}, time of maximum concentration; $t_{1/2}$, elimination half-life, i.v., intravenous; i.p., intraperitoneal.

Abstract

5-Methoxy-*N*,*N*,-dimethyltryptamine (5-MeO-DMT), an abused serotonergic indolealkylamine drug, has been placed into Schedule I controlled substance in the United States since January 19, 2011. Previously we have shown the impact of monoamine oxidase-A and cytochrome P450 2D6 enzymes in 5-MeO-DMT metabolism and pharmacokinetics. This study aimed to investigate 5-MeO-DMT pharmacokinetic properties following intravenous (i.v.) or intraperitoneal (i.p.) administration of three different doses (2, 10 and 20 mg/kg) to *CYP2D6*-humanized (Tg-*CYP2D6*) and wild-type control mice. The systemic exposure (AUC) to 5-MeO-DMT was increased non-proportionally with the increase of dose. The existence of nonlinearity in serum 5-MeO-DMT pharmacokinetics was clearly manifested by dose normalized AUC values, which were approximately 1.5 to 2.0-fold (i.v.) and 1.8 to 2.7-fold (i.p.) higher in wild-type or Tg-*CYP2D6* mice dosed with 10 and 20 mg/kg of 5-MeO-DMT, respectively, than those in mice treated with 2 mg/kg of 5-MeO-DMT. Furthermore, a two-compartment model including first-order absorption, nonlinear (Michaelis-Menten) elimination and CYP2D6-dependent linear elimination from central compartment was developed to characterize the i.v. and i.p. pharmacokinetic data of 5-MeO-DMT in wild-type and Tg-*CYP2D6* mice. In addition, 5-MeO-DMT was readily detected in mouse brain following drug treatment, and brain 5-MeO-DMT concentrations were also increased non-proportionally with the increase of dose. The results establish a nonlinear pharmacokinetic property for 5-MeO-DMT in mice, suggesting that risk of 5-MeO-DMT intoxication may be increased non-proportionally at higher doses.

DMD Fast Forward. Published on April 4, 2011 as DOI: 10.1124/dmd.111.039107
This article has not been copyedited and formatted. The final version may differ from this version.

Introduction

5-Methoxy-*N*,*N*-dimethyltryptamine (5-MeO-DMT), a psychoactive indolealkylamine derivative, is present in a variety of plant and animal preparations used for social or recreational purposes (Ott, 2001; Brandt et al., 2004; McKenna, 2004; Yu, 2008; Shen et al., 2010a; McIlhenny et al., 2011). As a potent, fast-acting hallucinogen with short duration, 5-MeO-DMT produces psychedelic effects in humans following different routes of administration, e.g., inhalation, intravenous (i.v.) injection, sublingual or intranasal insufflation, or oral administration with an inhibitor of monoamine oxidase-A (MAO-A). Human self-experiments have revealed that visionary threshold can be induced by insufflating or sublingual ingestion of 10 mg of 5-MeO-DMT free base (equal to 0.14 mg/kg) (Ott, 2001). The hallucination begins at 3-4 min, peaks around 35-40 min, and ends about 60-70 min after insufflation of 5-MeO-DMT free base. It is noteworthy that 5-MeO-DMT has been a controlled substance in European countries for years, while it becomes a Schedule I controlled substance in the United State since January 19, 2011 (DEA-2010-0024, 2010). Before that, 5-MeO-DMT was available on the Internet as natural products or synthetic compound. 5-MeO-DMT intoxications were also documented (Brush et al., 2004; Sklerov et al., 2005), and the symptoms included extremely high body temperature and heart rate, as well as combative hallucinating without vital sign. Particular attention (Sklerov et al., 2005; Callaway et al., 2006) is drawn to a fatal case that a strikingly high concentration of 5-MeO-DMT was found in the decedent's heart blood.

The toxicity of 5-MeO-DMT has been studied in different animal models including mouse, rat, sheep and monkey (Benington et al., 1965; Gillin et al., 1976). Following the treatment with 5-MeO-DMT, animals often show hyperthermia, ataxia, mydriasis, tremor, convulsion, shivering and salivation. While the LD_{50} of 5-MeO-DMT ranges from 48 to 278 mg/kg for different routes of administration to mice (Benington et al., 1965; Gillin et al., 1976), exposure to 1 mg/kg of 5-MeO-DMT causes severe toxic effects to sheep (Gillin et al., 1976). The species difference may be attributed to the differences in its metabolism and pharmacokinetics in individual animal models besides animal physiology, which hampers the prediction of 5-MeO-DMT toxicity in humans. Therefore, understanding pharmacokinetic properties across species is critical for proper correlation of drug exposure with drug effect, and ultimately, extrapolation of animal data to humans (Rhomberg, 1995; Green et al., 2009; Jiang et al., 2011).

Unfortunately there is no report on 5-MeO-DMT pharmacokinetics in humans. Limited pharmacokinetic studies using mouse or rat models suggest that 5-MeO-DMT is rapidly absorbed and eliminated (Sitaram et al., 1987a; Sitaram et al., 1987b; Shen et al., 2009; Shen et al., 2010b). The low urinary recovery and biliary excretion of substrate drug indicate that 5-MeO-DMT is predominantly eliminated through metabolism (Agurell et al., 1969; Sitaram et al., 1987a). *In vitro* and *in vivo* studies show that MAO-A-mediated deamination is the major metabolic pathway for 5-MeO-DMT, while other metabolic pathways like *N*-oxygenation, *N*-demethylation, *O*-demethylation were also reported (Agurell et al., 1969; Squires, 1975; Sitaram et al., 1987a; Sitaram et al., 1987b; Shen et al., 2009; Shen et al., 2010b). The *O*-demethylation mediated by CYP2D6 produces an

active metabolite bufotenine (Yu et al., 2003a). In addition, each study on the metabolism and disposition of 5-MeO-DMT is limited to a single dose (Agurell et al., 1969; Sitaram et al., 1987a; Sitaram et al., 1987b; Barker et al., 2001; Shen et al., 2009; Shen et al., 2010b). Therefore, this study investigated 5-MeO-DMT pharmacokinetics in mice at multiple dose levels and through different routes of administration, which cover the range from non-toxic to toxic dose levels, aiming to define the pharmacokinetic properties of 5-MeO-DMT, delineate the impact of CYP2D6 on systemic clearance of 5-MeO-DMT, and develop a pharmacokinetic model to quantitatively characterize serum concentration-time profiles of 5-MeO-DMT.

DMD Fast Forward. Published on April 4, 2011 as DOI: 10.1124/dmd.111.039107
This article has not been copyedited and formatted. The final version may differ from this version.

Materials and Methods

Chemical and Materials. 5-MeO-DMT oxalate and 5-methyl-*N*,*N*-dimethyltryptamine (5-Me-DMT) were purchased from Sigma-Aldrich (St. Louis, MO). Saline was bought from Henry-Schein (Melville, NY). All other reagents or organic solvents were either analytical or high-performance liquid chromatography (HPLC) grade (VWR, Bridgeport, NJ).

Animals. Wild-type FVB/N and *CYP2D6*-humanized (Tg-*CYP2D6*) mice (Corchero et al., 2001) were housed under the controlled temperature (20 ± 2°C), relative humidity (50-60%) and 12-h light/dark cycles with food and water provided *ad libitum*. Age-matched male adult mice (8 weeks old) weighting 25-30 g were used in the experiments. All animal procedures were approved by the Institutional Animal Care and Use Committee (IACUC) at University at Buffalo, SUNY.

Pharmacokinetic Studies. 5-MeO-DMT oxalate was dissolved in saline to a 10 mg/mL drug stock solution and further diluted with saline to appropriate concentrations that were utilized at 10 μL/g of body weight for i.p. doses and 5 μL/g of body weight for i.v. doses, respectively. Wild-type or Tg-*CYP2D6* mice were treated i.p. or i.v. with 2, 10 or 20 mg/kg of 5-MeO-DMT. Blood samples were collected from individual mice at different time points (0-180 min, N = 3 or 4 per time point) following the administration of 5-MeO-DMT. Serum was isolated with a serum separator (Becton Dickinson, Franklin Lakes, NJ) and stored at -80°C before analysis.

Brain Drug Distribution. Following i.p. treatment of 2, 10 or 20 mg/kg of 5-MeO-DMT, wild-type or Tg-*CYP2D6* mice were sacrificed at 20, 30 or 60 min. Brain tissues were excised, rinsed and homogenized with ice-cold saline. The homogenate were stored at -80°C for less than one year before analysis.

Liquid Chromatography Tandem Mass Spectrometry (LC-MS/MS) Quantification. A simple protein precipitation method was employed for the processing of serum samples. Ice-cold acetonitrile (60 µL) containing 50 nM of 5-Me-DMT (internal standard) was added to serum sample (20 µL) for protein precipitation. After centrifugation at 14,000 g for 10 min, the supernatant was injected for LC-MS/MS analysis.

The brain samples were subjected to liquid-liquid extraction. Brain homogenate (50 µL) was mixed with 10 µL of 5-Me-DMT (100 nM) and 5 µL of sodium hydroxide (1 M), and extracted with 1 mL of ethyl acetate. After centrifugation at 14,000 rpm for 5 min, 900 µL of supernatant was transferred to a new vial and evaporated to dryness under a stream of air. The residue was reconstituted with 50 µL of 50% methanol, and centrifuged at 14,000 rpm for 5 min. The supernatant was injected for LC-MS/MS analysis.

LC-MS/MS quantification of 5-MeO-DMT in mouse serum and brain samples was carried out using a Shimadzu prominence HPLC (Kyoto, Japan) coupled to an API 3000 turbo ionspray ionization triple-quadrupole mass spectrometer (Applied Biosystems, Foster City, CA). 5-MeO-DMT was separated from internal standard on a 3 µm

DMD Fast Forward. Published on April 4, 2011 as DOI: 10.1124/dmd.111.039107
This article has not been copyedited and formatted. The final version may differ from this version.

Phenomenex phenyl-hexyl column (50 × 4.6 mm, Torrance, CA), and quantified with the validated method (Shen et al., 2009). Brain 5-MeO-DMT concentrations were converted to ng/g based on the weights of individual mouse brain tissues.

Pharmacokinetic Modeling. Noncompartmental analysis was conducted using composite mean serum concentration-time data obtained from wild-type or Tg-*CYP2D6* mice at each dose level with WinNonLin (version 5.3, Pharsight, Mountain View, CA). The maximum serum drug concentration (C_{max}) and the time it occurred (T_{max}) after i.p. administration were recorded as observed. The area under serum drug concentration versus time curve up to the last measured time point ($AUC_{0\rightarrow t}$) was calculated by the trapezoidal rule, and the $AUC_{0\rightarrow\infty}$ was estimated by extrapolating the $AUC_{0\rightarrow t}$ to infinity using the last measured concentration and the terminal slope (λ) of linear regression from semi-logarithmic drug concentration versus time curve. The elimination half-life ($t_{1/2}$) was determined by the relationship of $0.693/\lambda$. The clearance (CL) was calculated by dose/$AUC_{0\rightarrow\infty}$, and the volume of distribution at steady state (Vss) was determined as CL times AUMC over AUC, where AUMC was the area under the first moment curve. Oral bioavailability (F) was estimated as the ratio of $AUC_{0\rightarrow\infty}$ values following i.p. and i.v. administration.

A compartmental model (Fig. 1) was proposed to describe 5-MeO-DMT data. Serum 5-MeO-DMT concentration-time data from wild-type and Tg-*CYP2D6* mice following i.v. and i.p. administrations were fit simultaneously to this model (Fig. 1) with ADAPT VI (BMSR, University of South California, Los Angeles, CA) by a naïve-pooled population

DMD Fast Forward. Published on April 4, 2011 as DOI: 10.1124/dmd.111.039107
This article has not been copyedited and formatted. The final version may differ from this version.

analysis. The initial estimates of model parameters were obtained from noncompartmental analysis. Model parameters were estimated with the maximum likelihood estimation method. Different models with or without peripheral compartment, with linear or nonlinear distribution or elimination were also tested. The final model (Fig. 1) was selected based on the goodness-of-fit criteria that included Akaike Information Criterion (AIC), estimation criterion value for the maximum likelihood method, and visual inspection of fitted profiles.

The differential equations of the final model were as follows:

$$\frac{dXa}{dt} = -ka \times Xa \qquad \text{(IC = F x Dose)} \tag{1}$$

$$\frac{dX_C}{dt} = ka \times Xa - \frac{V_{\max} \times X_C}{K_m \times V_C + X_C} + CL_D \times \frac{X_T}{V_T} \quad \text{(IC = 0)} \tag{2}$$

$$\frac{dX_C}{dt} = ka \times Xa - \frac{V_{\max} \times X_C}{K_m \times V_C + X_C} - CL_{CYP2D6} \times \frac{X_C}{V_C} + CL_D \times \frac{X_T}{V_T} \quad \text{(IC = 0)} \tag{3}$$

$$\frac{dX_C}{dt} = -\frac{V_{\max} \times X_C}{K_m \times V_C + X_C} + CL_D \times \frac{X_T}{V_T} \quad \text{(IC= Dose)} \tag{4}$$

$$\frac{dX_C}{dt} = -\frac{V_{\max} \times X_C}{K_m \times V_C + X_C} - CL_{CYP2D6} \times \frac{X_C}{V_C} + CL_D \times \frac{X_T}{V_T} \quad \text{(IC= Dose)} \tag{5}$$

$$\frac{dX_T}{dt} = CL_D \times (\frac{X_C}{V_C} - \frac{X_T}{V_T}) \quad \text{(IC = 0)} \tag{6}$$

The initial condition (IC) for each equation was provided in the parenthesis. Equations (1), (2), and (6) were used to fit the i.p. data from wild-type mice. Equations (1), (3), and

DMD Fast Forward. Published on April 4, 2011 as DOI: 10.1124/dmd.111.039107
This article has not been copyedited and formatted. The final version may differ from this version.

(6) were used to fit the i.p. data from Tg-*CYP2D6* mice. Equations (4) and (6) were used to fit the i.v. data from wild-type mice, and Equations (5) and (6) were used to fit the i.v. data from Tg-*CYP2D6* mice. In the equations, Xa represents the amount of 5-MeO-DMT at absorption site, and X_C and X_T represent the amount of 5-MeO-DMT in central and peripheral compartment, respectively. The ka is the absorption rate constant at absorption site, and F is the bioavailability. CL_D is the distribution clearance. V_C and V_T represent the volume of distribution of 5-MeO-DMT in the central and peripheral compartment, respectively. K_m is the Michaelis-Menten constant of the nonlinear elimination from central compartment, and V_{max} is the maximum velocity. CL_{CYP2D6} represents the additional linear clearance of 5-MeO-DMT from central compartment that is dependent on CYP2D6 protein and thus occurs only in Tg-*CYP2D6* mice.

Statistical Analyses. Statistical analysis was conducted using Student's t-test or one-way ANOVA followed by a Bonferroni's post hoc test (GraphPad Prism 5, GraphPad Software Inc., San Diego, CA). Difference was considered statistically significant when *P* value was less than 0.05 ($P < 0.05$).

Results

LC-MS/MS method was developed for quantification of serum and brain 5-MeO-DMT concentrations. A LC-MS/MS method coupled with protein precipitation (Shen et al., 2009) has been developed and validated for quantification of 5-MeO-DMT in serum samples. This method was optimized for the measurement of brain 5-MeO-DMT in this study. In particular, a liquid-liquid extraction method instead of protein precipitation was used for brain sample preparation. The recovery of 5-MeO-DMT was in the range of 62-70%. The lowest limit of quantification of 5-MeO-DMT was 4.1 nM, and standard curve ranged from 4.1 to 3000 nM with a linear regression coefficient over 0.99. The inter-day accuracy and precision were 99-106% and 3.7-9.6% for quality control samples at concentrations of 12.3, 111, 1000 nM. Similar as the method for quantification of serum samples, the analysis of 5-MeO-DMT or 5-Me-DMT (internal standard) in brain samples did not experience any ion-suppression or enhancement caused by the co-eluted matrix (data not shown). In addition, our pilot study showed that 5-MeO-DMT in brain homogenate was stable at -80°C for over one year, which was longer than the storage time of the brain samples. The methods were selective, sensitive, and able to quantify blood and brain 5-MeO-DMT concentrations in mice treated with drug, whereas endogenous 5-MeO-DMT in untreated mice was below the quantification limit.

Blood 5-MeO-DMT showed nonlinear pharmacokinetics following intravenous bolus administration. After quantification of 5-MeO-DMT, serum 5-MeO-DMT concentration-time curves were established (Fig. 2A and 2B). Noncompartmental analyses were first conducted to estimate 5-MeO-DMT pharmacokinetic parameters in

DMD Fast Forward. Published on April 4, 2011 as DOI: 10.1124/dmd.111.039107
This article has not been copyedited and formatted. The final version may differ from this version.

wild-type (Table 1) and Tg-*CYP2D6* (Table 2) mice. 5-MeO-DMT pharmacokinetic parameters (e.g., $AUC_{0\rightarrow\infty}$, CL, Vss and $t_{1/2}$) were not significantly different between wild-type (47.6 μmol·min/L, 0.19 L/min/kg, 2.27 L/kg and 9.2 min, respectively) and Tg-*CYP2D6* (49.1 μmol·min/L, 0.19 L/min/kg, 2.55 L/kg and 8.4 min, respectively) mice, indicating a limited role for CYP2D6 in systemic clearance of 5-MeO-DMT. Interestingly, change in $AUC_{0\rightarrow\infty}$ was greater than proportional increase in both genotyped mice (Tables 1 and 2). When the doses were increased to 10 and 20 mg/kg, the $AUC_{0\rightarrow\infty}$ values were increased to 487 and 920 μmol·min/L in wild-type mice, and 369 and 866 μmol·min/L in Tg-*CYP2D6* mice, respectively. While the dose-normalized $AUC_{0\rightarrow\infty}$ values for 10 mg/kg and 20 mg/kg were comparable, each was much higher than that for 2 mg/kg dose (2.0 and 1.9-fold higher in wild-type mice, and 1.5 and 1.8-fold higher in Tg-*CYP2D6* mice, respectively). Consistently, systemic clearance (CL) of 5-MeO-DMT at higher dose (10 or 20 mg/kg) was approximately 50% lower than that at low dose (2 mg/kg), and the half-life ($t_{1/2}$) at higher dose (10 or 20 mg/kg) was 30-63% longer than that at low dose (2 mg/kg) in wild-type and Tg-*CYP2D6* mice (Tables 1 and 2). The existence of nonlinearity in serum 5-MeO-DMT pharmacokinetics was also manifested by the dose-normalized serum drug concentration-time curves of 2 mg/kg doses (Fig. 2C and 2D), which did not superimpose with those of 10 mg/kg and 20 mg/kg doses in both wild-type and Tg-*CYP2D6* mice.

It should be noted that the use of oxalate salt did not affect the pharmacokinetics of 5-MeO-DMT in mice. This was confirmed by our pilot studies, showing that similar

DMD Fast Forward. Published on April 4, 2011 as DOI: 10.1124/dmd.111.039107
This article has not been copyedited and formatted. The final version may differ from this version.

pharmacokinetic profiles of 5-MeO-DMT were observed in mice receiving 5-MeO-DMT free base or 5-MeO-DMT oxalate (data not shown).

Nonlinear pharmacokinetics was also observed for blood 5-MeO-DMT following intraperitoneal administration. After i.p. administration, 5-MeO-DMT was readily absorbed with a C_{max} around 3-5 min in wild-type and Tg-*CYP2D6* mice (Fig. 3A and 3B, and Tables 1 and 2). The $AUC_{0\rightarrow\infty}$ values were 24.9, 231 and 654 μmol·min/L for 2, 10, and 20 mg/kg of 5-MeO-DMT in wild-type mice, respectively, and 20.9, 225 and 569 μmol·min/L for 2, 10, and 20 mg/kg of 5-MeO-DMT in Tg-*CYP2D6* mice, respectively. Consistent with the finding from i.v. administration, the increase of $AUC_{0\rightarrow\infty}$ with dose was greater than proportional change. In particular, the dose-normalized $AUC_{0\rightarrow\infty}$ values at 10 and 20 mg/kg dose were 1.9- and 2.6-fold higher, respectively, than that at 2 mg/kg dose in wild-type mice, and 2.2- and 2.7-fold higher, respectively, than that at 2 mg/kg dose in Tg-*CYP2D6* mice. Furthermore, the dose normalized C_{max} at higher dose (10 or 20 mg/kg) were 7-80% higher than that at 2 mg/kg in mice (Tables 1 and 2). In addition, the dose normalized serum drug concentration-time curve of 2 mg/kg dose did not superimpose with those of higher doses (10 and 20 mg/kg) in either wild-type or Tg-*CYP2D6* mice (Fig. 3C and 3D). The results indicated that 5-MeO-DMT pharmacokinetics in mice was nonlinear.

A compartmental model was developed to describe 5-MeO-DMT concentration-time profiles. To better understand 5-MeO-DMT pharmacokinetic properties, the serum 5-MeO-DMT concentration-time data after i.v. and i.p. administration were simultaneously

DMD Fast Forward. Published on April 4, 2011 as DOI: 10.1124/dmd.111.039107
This article has not been copyedited and formatted. The final version may differ from this version.

analyzed with ADAPT V. A number of different pharmacokinetic models, including one- or two-compartments with linear or Michaelis-Menten elimination, were first tested for the i.v. data. One-compartment model with linear elimination failed to capture the 5-MeO-DMT data. The change from linear to Michaelis-Menten elimination or the addition of a peripheral compartment under-predicted the concentrations of 5-MeO-DMT at early time points in mice receiving 10 and 20 mg/kg doses (data not shown). A two-compartment model with Michaelis-Menten elimination plus a CYP2D6-dependent linear elimination from central compartment provided the best fitting, according to the goodness-of-fit criteria. Therefore, a compartmental model (Fig. 1) was developed for simultaneously fit of the i.v. and i.p. pharmacokinetic data, which included a dosing compartment with linear first-order absorption rate. This model nicely captured the serum drug concentration-time data at different i.v. and i.p. doses in both wild-type and Tg-*CYP2D6* mice (Fig. 4), which is also evident from Goodness-of-fit plots (Fig. 5). The estimated compartmental pharmacokinetic parameters for 5-MeO-DMT were shown in Table 3. The ka value was 0.13 min^{-1}, suggesting that 5-MeO-DMT was rapidly absorbed after i.p. administration. According to the V_{max} and K_m values (2.76 μmol/min/kg and 13.2 μM, respectively), intrinsic clearance (CL_{int}) of 5-MeO-DMT from central compartment would be 0.21 L/min/kg, which was close to the systemic clearance value at 2 mg/kg dose obtained by noncompartmental analyses (Tables 1 and 2), and agreed with a linear elimination of 5-MeO-DMT at the low dose. In contrast, a low CL_{CYP2D6} value (0.0256 L/min/kg) in Tg-*CYP2D6* mice supported that CYP2D6-mediated *O*-demethylation was a minor pathway in systemic elimination of 5-MeO-DMT. Overall,

this compartmental model (Fig. 1) provided reasonable description of 5-MeO-DMT pharmacokinetic data (Fig. 4) in mice.

5-MeO-DMT exhibited nonlinear accumulation in mouse brain following i.p. drug administration. Since 5-MeO-DMT acts on the central nervous system (CNS), we further measured brain 5-MeO-DMT concentrations at 20, 30 and 60 min following i.p. drug administration. Compared with serum drug concentrations at the same time point, brain 5-MeO-DMT concentrations were much higher. For instance, the brain/serum ratios of 5-MeO-DMT concentrations ranged from 1.8 to 4.1 in wild-type mice, and from 1.2 to 4.2 in Tg-*CYP2D6* mice treated with 10 mg/kg of drug. When dosed with 20 mg/kg of 5-MeO-DMT, the ratios were 2.7-4.3 and 3.2-5.2 in wild-type and Tg-*CYP2D6* mice, respectively. Most importantly, 5-MeO-DMT concentrations increased non-proportionally in brain with the increase of dose, similar to the nonlinear pharmacokinetics observed for blood 5-MeO-DMT (Fig. 2 and 3). Therefore, the dose normalized brain 5-MeO-DMT concentrations were calculated (Fig. 6), which were about 3- to 11-fold higher at 20 min, 3- to 14-fold higher at 30 min, and 2- to 16-fold higher at 60 min, respectively, in mice dosed with 10 or 20 mg/kg of drug than those dosed with 2 mg/kg of drug. The results indicated a nonlinear accumulation of 5-MeO-DMT in mouse brain.

Discussion

Current study reveals a nonlinear pharmacokinetics for 5-MeO-DMT, a new Schedule I controlled substance in the United States (DEA-2010-0024, 2010), in mouse model following intravenous and intraperitoneal drug administration (Fig. 2 and 3). Although the experiments were not designed for studying toxicological effects, we did observe significant behavior changes and toxic syndromes in mice receiving higher doses (10 and 20 mg/kg) of 5-MeO-DMT. The decrease (~50%) of systemic clearance at higher doses indicates the presence of nonlinearity in 5-MeO-DMT elimination. Given the facts that metabolic elimination is the major elimination pathway for 5-MeO-DMT and MAO-A-mediated deamination is the main metabolic pathway for 5-MeO-DMT (Agurell et al., 1969; Squires, 1975; Suzuki et al., 1981; Sitaram et al., 1987b; Shen et al., 2009; Shen et al., 2010b), saturation of MAO-A-mediated metabolic elimination is presumably the cause of nonlinear clearance of 5-MeO-DMT.

Nonlinear pharmacokinetics has been documented for other drugs of abuse in different species. An amphetamine drug of abuse, 3,4-methylenedioxymetham-phetamine (MDMA, "ecstasy"), exhibits nonlinear pharmacokinetics in rodents, nonhuman primates, and humans, which may influence the likelihood and severity of MDMA toxicities (de la Torre et al., 2000; Mueller et al., 2008; Baumann et al., 2009). Current study clearly demonstrates a nonlinear pharmacokinetics for 5-MeO-DMT in mice (Fig. 2 and 3), which may complicate the prediction of 5-MeO-DMT toxicity. In general, the nonlinear pharmacokinetics leads to a much narrower range between safe and toxic doses, and makes it more difficult in extrapolation of dose-effect or dose-toxicity relationship (Tonn

et al., 2009; Lledo-Garcia et al., 2010). Thus the development of appropriate quantitative model may offer better understanding of pharmacokinetic properties in support of pharmacological and toxicological investigations.

The calculated systemic clearance for 5 -MeO-DMT (0.094-0.19 L/min/kg from noncompartmental analyses; Tables 1 and 2) is close or higher than hepatic blood flow in mice (90 mL/min/kg) (Davies and Morris, 1993), suggesting the existence of extrahepatic elimination. Indeed, MAO-A enzyme is expressed in many extrahepatic tissues, e.g., gut, kidney, lung and myocardium (Thorpe et al., 1987; Saura et al., 1996), which likely contributes to the metabolic elimination of 5-MeO-DMT. The volume of distribution (Vss) of 5-MeO-DMT in mice is 1.68-2.55 L/kg, which is much higher than the volume of blood and total body water of mouse with a body weight of 20 g (0.81 L/kg) (Davies and Morris, 1993), indicating an extensive binding of 5-MeO-DMT to the tissues. Accumulation of 5-MeO-DMT in animal tissues is supported by its high lipophilicity (partition coefficient = 3. 30) (Glennon and Gessner, 1979), and it is also evident from previous studies in rats (Sitaram and McLeod, 1990).

The two-compartment pharmacokinetic model (Fig. 1) developed for 5-MeO-DMT in current study provides good rationalization of the i.v. and i.p. data in mice (Fig. 4 and 5). The capacity-limited elimination of 5-MeO-DMT (K_m, V_{max}) from central compartment explains well the nonlinear profiles after i.v. and i.p. administrations (Fig. 2 and 3), and the simulated clearance values (Supplemental Fig. 1) show a clear tread of decrease in drug clearance with the increase of dose in both wild-type and transgenic mice,

supporting a nonlinear pharmacokinetics for 5-MeO-DMT. The estimated K_m value (13.2 μM) is close to the reported K_m value for deamination of tryptamine analogs (including 5-MeO-DMT) by MAO-A enzyme (Squires, 1975; Suzuki et al., 1981; Yu et al., 2003b). Since mouse serum 5-MeO-DMT concentrations after 2 mg/kg i.v. dose are much lower than the estimated K_m value, MAO-mediated elimination of drug at this dose should be still in linear range. Therefore, 5-MeO-DMT at dose levels lower than 2 mg/kg could be in a linear kinetic range, which is supported by simulated results (data not shown). In contrast, serum 5-MeO-DMT concentrations at earlier time points following higher doses (10 or 20 mg/kg) of drug (Fig. 2 and 3) are much higher than the K_m value, and thus MAO-mediated elimination could be saturated, leading to the nonlinear drug elimination, as compared to lower (e.g., 2 mg/kg) doses. On the other hand, CYP2D6 is revealed to play a minor role in elimination of 5-MeO-DMT *in vivo*, as indicated by the CL_{CYP2D6} value that is only around 10% of the intrinsic clearance (V_{max}/K_m) (Table 3). Nevertheless, it is unknown if CYP2D6-mediated metabolism (Yu et al., 2003a) would compensate to the clearance of 5-MeO-DMT when MAO-A activity is inhibited.

5-MeO-DMT is a nonselective serotonin (5-HT) receptor agonist. 5-HT_{1A} and 5-HT_2 receptors have been shown to determine the complex pharmacological and toxicological actions of 5-MeO-DMT at CNS (Winter et al., 2000; Krebs-Thomson et al., 2006; Halberstadt et al., 2008). Understanding brain 5-MeO-DMT concentrations would be helpful. Our pilot study has shown that 5-MeO-DMT concentrations in different mouse brain regions, e.g., hippocampus, hypothalamus, striatum and cortex, are comparable (data not shown). This study, therefore, focuses on measurement of 5-MeO-DMT

concentrations in the whole brain following i.p. administration. Consistent with previous findings (Barker et al., 2001), 5-MeO-DMT is capable to penetrate blood-brain barrier and accumulate within animal brains. The most significant finding is the greater than proportional increase of brain 5-MeO-DMT concentration with the increase of dose (Fig. 6). Agreeing with the nonlinear pharmacokinetics of blood 5-MeO-DMT (Fig. 2 and 3), the nonlinear accumulation of 5-MeO-DMT in brain tissue illustrates an increased risk of 5-MeO-DMT intoxication at higher doses.

In summary, 5-MeO-DMT exhibits nonlinear pharmacokinetics in mice following intravenous and intraperitoneal administration. A two-compartment pharmacokinetic model with linear absorption and capacity-limited elimination, as well as a minor metabolic elimination by CYP2D6, well characterizes the pharmacokinetic profiles of 5-MeO-DMT in wild-type and Tg-*CYP2D6* mice. These findings may serve as a basis for further investigation of the relationship between 5-MeO-DMT drug exposure and toxicity, particularly at doses when saturation of metabolic elimination occurs. In addition, 5-MeO-DMT is accumulated at a level greater than proportion in mouse brain, which increases the potential of 5-MeO-DMT toxicity. The results shall provide important insights into risk of 5-MeO-DMT intoxication, from the pharmacokinetic aspect.

Author Contributions:

Participated in research design: Shen and Yu

Conducted experiments: Shen and Jiang

Performed data analysis: Shen, Jiang and Yu

Wrote or contributed to the writing of the manuscript: Shen, Jiang and Yu

References:

Agurell S, Holmstedt B and Lindgren JE (1969) Metabolism of 5 -methoxy-N,-N dimethyltryptamine- 14 C in the rat. *Biochem Pharmacol* **18:**2771-2781.

Barker SA, Littlefield-Chabaud MA and David C (2001) Distribution of the hallucinogens N,N-dimethyltryptamine and 5-methoxy-N,N-dimethyltryptamine in rat brain following intraperitoneal injection: application of a new solid-phase extraction LC-APcI-MS-MS-isotope dilution method. *J Chromatogr B Biomed Sci Appl* **751:**37-47.

Baumann MH, Zolkowska D, Kim I, Scheidweiler KB, Rothman RB and Huestis MA (2009) Effects of dose and route of administration on pharmacokinetics of (+ or -)-3,4-methylenedioxymethamphetamine in the rat. *Drug Metab Dispos* **37:**2163-2170.

Benington F, Morin RD and Clark LC, Jr. (1965) 5-methoxy-N, N-dimethyltryptamine, a possible endogenous psychotoxin. *Ala J Med Sci* **2:**397-403.

Brandt SD, Freeman S, McGagh P, Abdul-Halim N and Alder JF (2004) An analytical perspective on favoured synthetic routes to the psychoactive tryptamines. *J Pharm Biomed Anal* **36:**675-691.

Brush DE, Bird SB and Boyer EW (2004) Monoamine oxidase inhibitor poisoning resulting from Internet misinformation on illicit substances. *J Toxicol Clin Toxicol* **42:**191-195.

Callaway JC, Grob CS, McKenna DJ, Nichols DE, Shulgin A and Tupper KW (2006) A demand for clarity regarding a case report on the ingestion of 5-methoxy-N, N-dimethyltryptamine (5-MeO-DMT) in an Ayahuasca preparation. *J Anal Toxicol* **30:**406-407; author reply 407.

Corchero J, Granvil CP, Akiyama TE, Hayhurst GP, Pimprale S, Feigenbaum L, Idle JR and Gonzalez FJ (2001) The CYP2D6 humanized mouse: effect of the human CYP2D6 transgene and HNF4alpha on the disposition of debrisoquine in the mouse. *Mol Pharmacol* **60:**1260-1267.

Davies B and Morris T (1993) Physiological parameters in laboratory animals and humans. *Pharm Res* **10:**1093-1095.

de la Torre R, Farre M, Ortuno J, Mas M, Brenneisen R, Roset PN, Segura J and Cami J (2000) Non-linear pharmacokinetics of MDMA ('ecstasy') in humans. *Br J Clin Pharmacol* **49:**104-109.

DEA-2010-0024 (2010) Schedules of Controlled Substances: Placement of 5-Methoxy-N,N-Dimethyltryptamine Into Schedule I of the Controlled Substances Act. *http://www.deadiversion.usdoj.gov/fed_regs/rules/2010/fr1220.htm*.

Gillin JC, Tinklenberg J, Stoff DM, Stillman R, Shortlidge JS and Wyatt RJ (1976) 5-Methoxy-N,N-dimethyltryptamine: behavioral and toxicological effects in animals. *Biol Psychiatry* **11:**355-358.

Glennon RA and Gessner PK (1979) Serotonin receptor binding affinities of tryptamine analogues. *J Med Chem* **22:**428-432.

Green AR, Gabrielsson J, Marsden CA and Fone KC (2009) MDMA: on the translation from rodent to human dosing. *Psychopharmacology (Berl)* **204:**375-378.

Halberstadt AL, Buell MR, Masten VL, Risbrough VB and Geyer MA (2008) Modification of the effects of 5-methoxy-N,N-dimethyltryptamine on exploratory

behavior in rats by monoamine oxidase inhibitors. *Psychopharmacology (Berl)* **201:**55-66.

Jiang XL, Gonzalez FJ and Yu AM (2011) Drug-metabolizing enzyme, transporter, and nuclear receptor genetically modified mouse models. *Drug Metab Rev* **43:**27-40.

Krebs-Thomson K, Ruiz EM, Masten V, Buell M and Geyer MA (2006) The roles of 5-HT1A and 5-HT2 receptors in the effects of 5-MeO-DMT on locomotor activity and prepulse inhibition in rats. *Psychopharmacology (Berl)* **189:**319-329.

Lledo-Garcia R, Nacher A, Casabo VG and Merino-Sanjuan M (2010) A pharmacokinetic model for evaluating the impact of hepatic and intestinal first-pass loss of saquinavir in the rat. *Drug Metab Dispos* **39:**294-301.

McIlhenny EH, Riba J, Barbanoj MJ, Strassman R and Barker SA (2011) Methodology for and the determination of the major constituents and metabolites of the Amazonian botanical medicine ayahuasca in human urine. *Biomed Chromatogr*.

McKenna DJ (2004) Clinical investigations of the therapeutic potential of a yahuasca: rationale and regulatory challenges. *Pharmacol Ther* **102:**111-129.

Mueller M, P eters FT, Maurer HH, McCann UD and Ricaurte GA (2008) Nonlinear pharmacokinetics of (+/-)3,4-methylenedioxymethamphetamine (MDMA, "Ecstasy") and its major metabolites in squirrel monkeys at plasma concentrations of MDMA that develop after typical psychoactive doses. *J Pharmacol Exp Ther* **327:**38-44.

Ott J (2001) Pharmepena-Psychonautics: Human intranasal, sublingual and oral pharmacology of 5-methoxy-N,N-dimethyl-tryptamine. *J Psychoactive Drugs* **33:**403-407.

Rhomberg L (1995) Use of quantitative modelling in methylene chloride risk assessment. *Toxicology* **102:**95-114.

Saura J, Nadal E, van den Berg B, Vila M, Bombi JA and Mahy N (1996) Localization of monoamine oxidases in human peripheral tissues. *Life Sci* **59:**1341-1349.

Shen HW, Jiang XL, Winter JC and Yu A M (2010a) Psychedelic 5-methoxy-N,N-dimethyltryptamine: metabolism, pharmacokinetics, drug interactions, and pharmacological actions. *Curr Drug Metab* **11:**659-666.

Shen HW, Jiang XL and Yu AM (2009) Development of a L C–MS/MS method to analyze 5-methoxy-N,N-dimethyltryptamine and bufotenine: application to pharmacokinetic study. *Bioanalysis* **1:**87-95.

Shen HW, Wu C, Jiang XL and Yu AM (2010b) Effects of monoamine oxidase inhibitor and cytochrome P450 2D6 status on 5-methoxy-N,N-dimethyltryptamine metabolism and pharmacokinetics. *Biochem Pharmacol* **80:**122-128.

Sitaram BR, Lockett L, Blackman GL and McLeod WR (1987a) Urinary excretion of 5-methoxy-N,N-dimethyltryptamine, N,N-dimethyltryptamine and their N-oxides in the rat. *Biochem Pharmacol* **36:**2235-2237.

Sitaram BR, Lockett L, Talomsin R, Blackman GL and McLeod WR (1987b) In vivo metabolism of 5 -methoxy-N,N-dimethyltryptamine and N,N-dimethyltryptamine in the rat. *Biochem Pharmacol* **36:**1509-1512.

Sitaram BR and McLeod WR (1990) Observations on th e metabolism of t he psychotomimetic indolealkylamines: implications for future clinical studies. *Biol Psychiatry* **28:**841-848.

Sklerov J, Levine B, Moore KA, King T and Fowler D (2005) A fatal intoxication following the ingestion of 5-methoxy-N,N-dimethyltryptamine in an ayahuasca preparation. *J Anal Toxicol* **29:**838-841.

Squires RF (1975) Evidence that 5-methoxy-N, N-dimethyl tryptamine is a specific substrate for MAO-A in the rat: implications for the indoleamine dependent behavioural syndrome. *J Neurochem* **24:**47-50.

Suzuki O, Katsumata Y and Oya M (1981) Characterization of eight biogenic indoleamines as substrates for type A and type B monoamine oxidase. *Biochem Pharmacol* **30:**1353-1358.

Thorpe LW, Westlund KN, Kochersperger LM, Abell CW and Denney RM (1987) Immunocytochemical localization of monoamine oxidases A and B in human peripheral tissues and brain. *J Histochem Cytochem* **35:**23-32.

Tonn GR, Wong SG, Wong SC, Johnson MG, Ma J, Cho R, Floren LC, Kersey K, Berry K, Marcus AP, Wang X, Van Lengerich B, Medina JC, Pearson PG and Wong BK (2009) An inhibitory metabolite leads to dose- and time-dependent pharmacokinetics of (R)-N-{1-[3-(4-ethoxy-phenyl)-4-oxo-3,4-dihydro-pyrido[2,3-d]pyrimidin-2-yl]-ethyl}-N-pyridin-3-yl-methyl-2-(4-trifluoromethoxy-phenyl)-acetamide (AMG 487) in human subjects after multiple dosing. *Drug Metab Dispos* **37:**502-513.

Winter JC, Filipink RA, Timineri D, Helsley SE and Rabin RA (2000) The paradox of 5-methoxy-N,N-dimethyltryptamine: an indoleamine hallucinogen that induces stimulus control via 5-HT1A receptors. *Pharmacol Biochem Behav* **65:**75-82.

Yu AM (2008) Indolealkylamines: biotransformations and potential drug-drug interactions. *Aaps J* **10:**242-253.

Yu AM, Idle JR, Herraiz T, Kupfer A and Gonzalez FJ (2003a) Screening for endogenous substrates reveals that CYP2D6 is a 5-methoxyindolethylamine O-demethylase. *Pharmacogenetics* **13:**307-319.

Yu AM, Granvil CP, Haining RL, Krausz KW, Corchero J, Kupfer A, Idle JR and Gonzalez FJ (2003b) The relative contribution of monoamine oxidase and cytochrome p450 isozymes to the metabolic deamination of the trace amine tryptamine. *J Pharmacol Exp Ther* **304:**539-546.

Footnotes:

This project was supported by National Institute On Drug Abuse, National Institutes of Health [Award Number R01DA021172].

Send reprint requests to: Dr. Ai-Ming Yu, University at Buffalo, The State University of New York, Buffalo, NY 14260-1200; Email: aimingyu@buffalo.edu.

Table 1. Pharmacokinetic parameters of 5-MeO-DMT in w ild-type mice following i.v. and i.p. administration determined by noncompartmental analyses.

	i.v. administration			i.p. administration		
	2 mg/kg	10 mg/kg	20 mg/kg	2 mg/kg	10 mg/kg	20 mg/kg
$AUC_{0\rightarrow\infty}$ (μmol·min/L)	47.6	487	920	24.9	231	654
$AUC_{0\rightarrow\infty}$/Dose (kg·min/L)	5.19	10.6	10.0	2.71	5.03	7.13
CL (L/min/kg)	0.19	0.094	0.10	---	---	---
V_{ss} (L/kg)	2.27	2.08	1.84	---	---	---
T_{max} (min)	---	---	---	3	5	5
C_{max} (μmol/L)	---	---	---	1.31	7.00	15.8
C_{max}/Dose (kg/L)	---	---	---	0.14	0.15	0.17
$T_{1/2}$ (min)	9.2	12	15	---	---	---
F (%)	---	---	---	52.2	47.3	71.0

Table 2. Pharmacokinetic parameters of 5-MeO-DMT in Tg-*CYP2D6* mice following i.v. and i.p. administration determined by noncompartmental analyses.

	i.v. administration			i.p. administration		
	2 mg/kg	10 mg/kg	20 mg/kg	2 mg/kg	10 mg/kg	20 mg/kg
$AUC_{0\rightarrow\infty}$ (μmol·min/L)	49.1	369	866	20.9	225	569
$AUC_{0\rightarrow\infty}$/Dose (kg·min/L)	5.36	8.10	9.45	2.28	4.92	6.20
CL (L/min/kg)	0.19	0.12	0.11	---	---	---
V_{ss} (L/kg)	2.55	1.68	2.18	---	---	---
T_{max} (min)	---	---	---	3	5	5
C_{max} (μmol/L)	---	---	---	1.01	8.93	18.3
C_{max}/Dose (kg/L)	---	---	---	0.11	0.19	0.20
$T_{1/2}$ (min)	8.4	12	12	---	---	---
F (%)	---	---	---	42.5	61.0	65.6

DMD Fast Forward. Published on April 4, 2011 as DOI: 10.1124/dmd.111.039107
This article has not been copyedited and formatted. The final version may differ from this version.

Table 3. Pharmacokinetic parameters of 5 -MeO-DMT following intravenous and intraperitoneal administration determined by compartmental analyses (Fig. 1).

Parameter	Unit	Estimated value	CV%
V_{max}	μmol/min/kg	2.76	0.028
K_m	μM	13.2	0.034
CL_D	L/min/kg	0.280	0.006
CL_{CYP2D6}	L/min/kg	0.0256	0.012
V_C	L/kg	1.34	0.005
V_T	L/kg	1.91	0.011
Ka	min^{-1}	0.131	0.005
F	%	81.3	0.004

DMD Fast Forward. Published on April 4, 2011 as DOI: 10.1124/dmd.111.039107
This article has not been copyedited and formatted. The final version may differ from this version.

Figure Legends

Figure 1. The pharmacokinetic model developed to describe serum 5-MeO-DMT concentration-time profiles in mice following i.v. and i.p. administration. Xa, amount of drug at the absorption site; K_a, absorption rate constant; F, bioavailability; X_C and X_T, amount of drug in central and peripheral compartment, respectively; V_C and V_T, volume of distribution of 5-MeO-DMT in central and peripheral compartment, respectively; K_m and V_{max}, Michaelis-Menten parameters for the saturable elimination of 5-MeO-DMT from central compartment; CL_{CYP2D6}, clearance of 5-MeO-DMT from central compartment by CYP2D6-dependent metabolism, which only occurs in Tg-*CYP2D6* mice; CL_D, distribution clearance of 5-MeO-DMT between central and peripheral compartments.

Figure 2. Serum 5-MeO-DMT concentration versus time curves in wild-type (A) and Tg-*CYP2D6* mice (B) following i.v. administration. Existence of nonlinear pharmacokinetics is manifested by the dose-normalized serum drug concentration versus time profiles in both wild-type (C) and Tg-*CYP2D6* mice (D). Mice were dosed intravenously with 2 (●), 10 (■) or 20 (▲) mg/kg of 5-MeO-DMT. Values are mean ± SD (N = 3 at each time point).

Figure 3. Serum 5-MeO-DMT concentration versus time curves in wild-type (A) and Tg-*CYP2D6* mice (B) following i.p. administration. Nonlinear pharmacokinetics is obvious from the dose-normalized serum drug concentration versus time profiles in wild-type (C)

and Tg-*CYP2D6* mice (D). Mice were treated intraperitoneally with 2 (●), 10 (■) or 20 (▲) mg/kg of 5-MeO-DMT. Values represent mean ± SD (N = 4 at each time point).

Figure 4. Simultaneous fitting of i.v. and i.p. pharmacokinetic data in both wild-type and Tg-*CYP2D6* mice using the proposed compartmental model (Fig. 1). Values are mean ± SD (N = 3-4 at each time point). Lines represent the predicted serum 5-MeO-DMT concentrations.

Figure 5. Goodness-of-fit plots of two-compartment model versus one-compartment model. Model predicted versus observed drug concentrations of one-compartment model (A) and final two-compartment model (B). Standard residuals vs. model predictions of one-compartment model (C) and final two-compartment model (D).

Figure 6. Dose normalized brain 5-MeO-DMT concentrations at 20 min after i.p. administrations of 2, 10 or 20 mg/kg of drug in wild-type and Tg-*CYP2D6* mice. Data are Mean ± SD (N = 4 in each group). $^{*}P < 0.05$, compared to 2 mg/kg treatment for the same genotype of mice, $^{\#}P < 0.05$, compared to wild-type mice treated with the same dose of drug.

Fig. 1

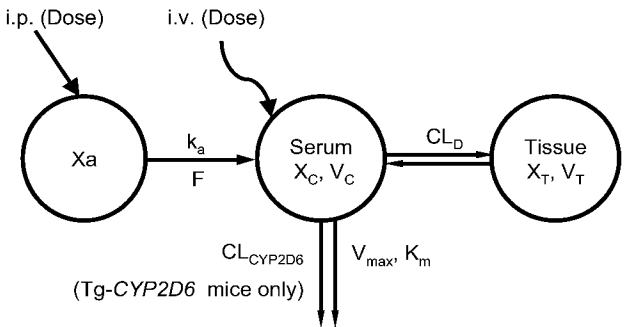
i.p. (Dose)
i.v. (Dose)
Xa
k_a
F
Serum
X_C, V_C
CL_D
Tissue
X_T, V_T
CL_{CYP2D6}
V_{max}, K_m
(Tg-*CYP2D6* mice only)

Fig. 2

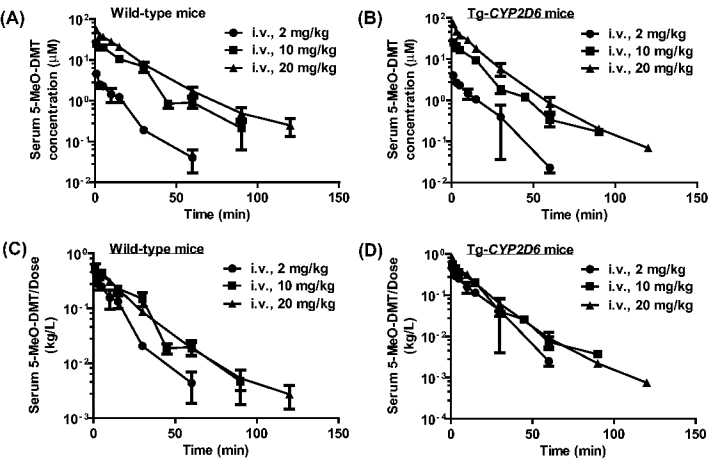
(A)
Wild-type mice
i.v., 2 mg/kg
i.v., 10 mg/kg
i.v., 20 mg/kg
Serum 5-MeO-DMT concentration (μM)
Time (min)
(B)
Tg-CYP2D6 mice
i.v., 2 mg/kg
i.v., 10 mg/kg
i.v., 20 mg/kg
Serum 5-MeO-DMT concentration (μM)
Time (min)
(C)
Wild-type mice
i.v., 2 mg/kg
i.v., 10 mg/kg
i.v., 20 mg/kg
Serum 5-MeO-DMT/Dose (kg/L)
Time (min)
(D)
Tg-CYP2D6 mice
i.v., 2 mg/kg
i.v., 10 mg/kg
i.v., 20 mg/kg
Serum 5-MeO-DMT/Dose (kg/L)
Time (min)

Fig. 3

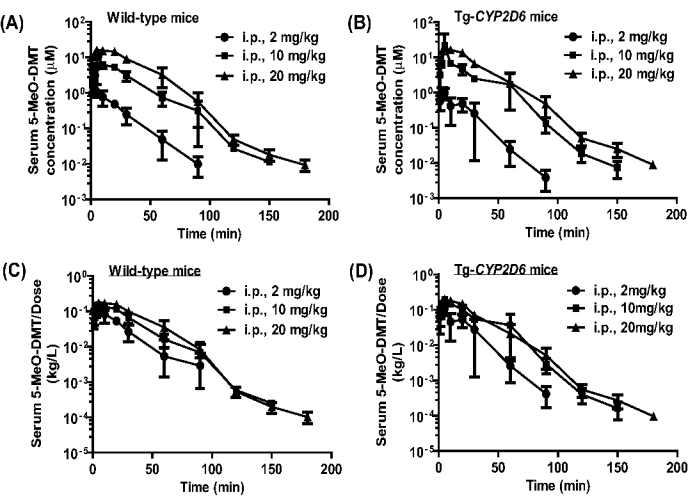
(A)
Wild-type mice
i.p., 2 mg/kg
i.p., 10 mg/kg
i.p., 20 mg/kg
Serum 5-MeO-DMT concentration (μM)
Time (min)
(B)
Tg-CYP2D6 mice
i.p., 2 mg/kg
i.p., 10 mg/kg
i.p., 20 mg/kg
Serum 5-MeO-DMT concentration (μM)
Time (min)
(C)
Wild-type mice
i.p., 2 mg/kg
i.p., 10 mg/kg
i.p., 20 mg/kg
Serum 5-MeO-DMT/Dose (kg/L)
Time (min)
(D)
Tg-CYP2D6 mice
i.p., 2mg/kg
i.p., 10mg/kg
i.p., 20mg/kg
Serum 5-MeO-DMT/Dose (kg/L)
Time (min)

Fig. 4

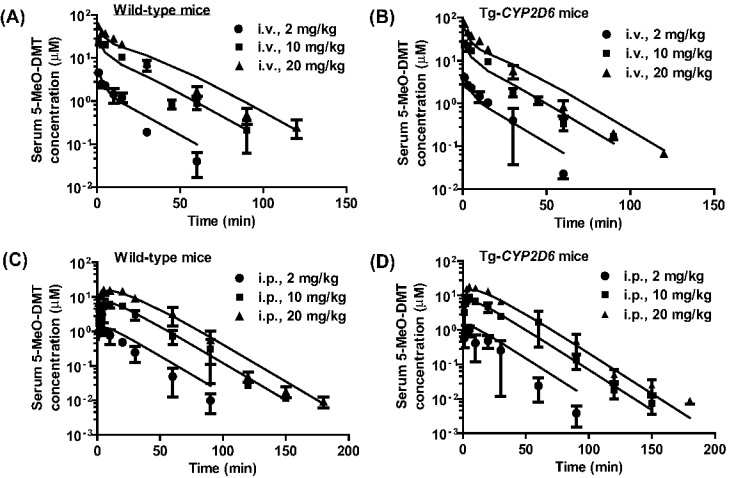
(A)
Wild-type mice
i.v., 2 mg/kg
i.v., 10 mg/kg
i.v., 20 mg/kg
Serum 5-MeO-DMT concentration (μM)
Time (min)
(B)
Tg-CYP2D6 mice
i.v., 2 mg/kg
i.v., 10 mg/kg
i.v., 20 mg/kg
Serum 5-MeO-DMT concentration (μM)
Time (min)
(C)
Wild-type mice
i.p., 2 mg/kg
i.p., 10 mg/kg
i.p., 20 mg/kg
Serum 5-MeO-DMT concentration (μM)
Time (min)
(D)
Tg-CYP2D6 mice
i.p., 2 mg/kg
i.p., 10 mg/kg
i.p., 20 mg/kg
Serum 5-MeO-DMT concentration (μM)
Time (min)

Fig. 5

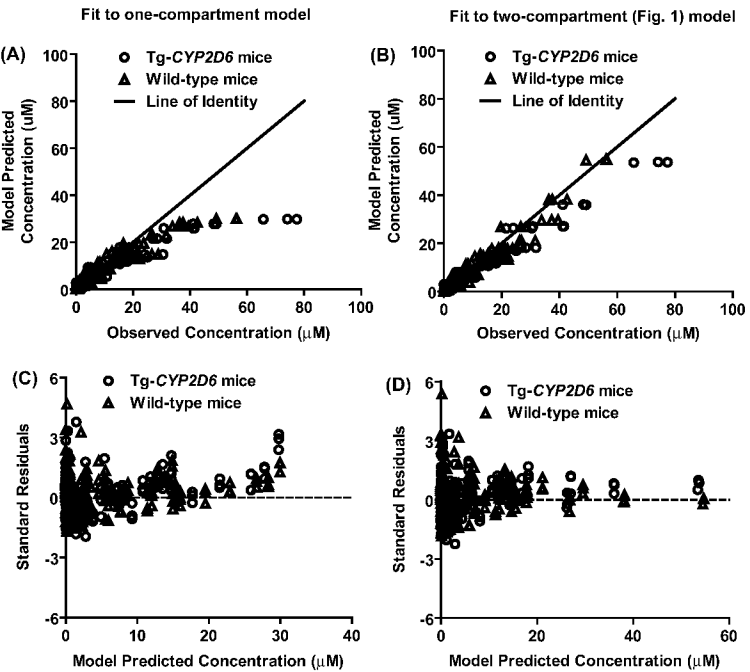
Fit to one-compartment model
Fit to two-compartment (Fig. 1) model
(A)
(B)
(C)
(D)
Tg-CYP2D6 mice
Wild-type mice
Line of Identity
Model Predicted Concentration (uM)
Observed Concentration (μM)
Standard Residuals
Model Predicted Concentration (μM)

Fig. 6

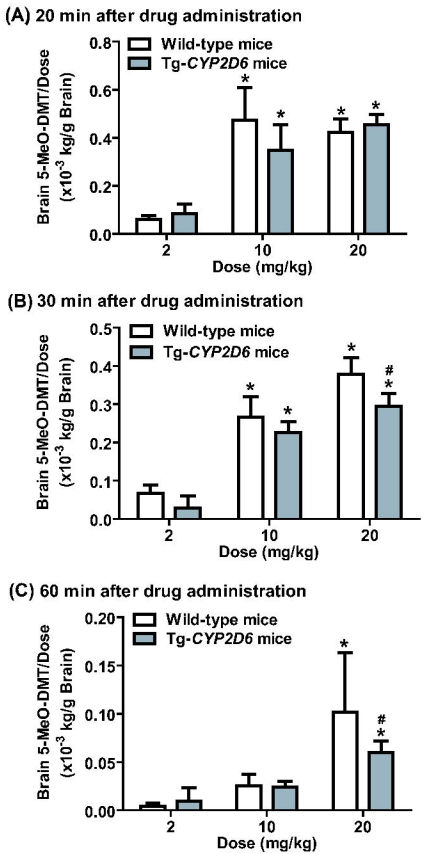
(A) 20 min after drug administration
Wild-type mice
Tg-CYP2D6 mice
Brain 5-MeO-DMT/Dose (x10-3 kg/g Brain)
0.8
0.6
0.4
0.2
0.0
2
10
20
Dose (mg/kg)
(B) 30 min after drug administration
Wild-type mice
Tg-CYP2D6 mice
Brain 5-MeO-DMT/Dose (x10-3 kg/g Brain)
0.5
0.4
0.3
0.2
0.1
0.0
2
10
20
Dose (mg/kg)
(C) 60 min after drug administration
Wild-type mice
Tg-CYP2D6 mice
Brain 5-MeO-DMT/Dose (x10-3 kg/g Brain)
0.20
0.15
0.10
0.05
0.00
2
10
20
Dose (mg/kg)